



Optimization of the Lead Compound NVP-BHG712 as a Colorectal Cancer Inhibitor

Alix Tröster^{+, [a]}, Michael DiPrima^{+, [b]}, Nathalie Jores,^[a] Denis Kudlinzki,^[a, c] Sridhar Sreeramulu,^[a] Santosh L. Gande,^[a, c] Verena Linhard,^[a] Damian Ludig,^[a] Alexander Schug,^[a] Krishna Saxena,^[a] Maria Reinecke,^[d, e] Stephanie Heinzlmeir,^[d] Matthias S. Leisegang,^[f] Jan Wollenhaupt,^[g] Frank Lennartz,^[g] Manfred S. Weiss,^[g] Bernhard Kuster,^[d, e, h] Giovanna Tosato,^{*, [b]} and Harald Schwalbe^{*, [a, c]}

Abstract: The ephrin type-A receptor 2 (EPHA2) kinase belongs to the largest family of receptor tyrosine kinases. There are several indications of an involvement of EPHA2 in the development of infectious diseases and cancer. Despite pharmacological potential, EPHA2 is an under-examined target protein. In this study, we synthesized a series of derivatives of the inhibitor NVP-BHG712 and triazine-based compounds. These compounds were evaluated to determine their potential as kinase inhibitors of EPHA2, including

elucidation of their binding mode (X-ray crystallography), affinity (microscale thermophoresis), and selectivity (Kino-beads assay). Eight inhibitors showed affinities in the low-nanomolar regime ($K_D < 10$ nM). Testing in up to seven colon cancer cell lines that express EPHA2 reveals that several derivatives feature promising effects for the control of human colon carcinoma. Thus, we have developed a set of powerful tool compounds for fundamental new research on the interplay of EPH receptors in a cellular context.

Introduction

Protein kinases have been a focus of medicinal chemistry as potential drug targets. Numerous inhibitors, both orthosteric and allosteric, have been developed. Many of these inhibitors are effective drugs approved for clinical applications. The ephrin type-A receptor 2 (EPHA2) is a less explored target despite its substantial pharmacological potential. The role of EPHA2 has been widely investigated in recent years, showing involvement

in infectious diseases and cancer.^[1,2] Overexpression of EPHA2 is observed in different cancer types (breast,^[3] head and neck,^[4] non-small-cell lung cancer^[5] and colorectal cancer (CRC)^[6]), and often predicts a poor clinical prognosis.^[6,7]

Several approaches have been exploited for targeting EPHA2, including agonistic^[8,9] as well as antagonistic^[10,11] acting small molecules and peptides. Two strategies for interfering with EPHA2 are commonly used: 1) Interaction with

[a] Dr. A. Tröster,⁺ N. Jores, Dr. D. Kudlinzki, Dr. S. Sreeramulu, Dr. S. L. Gande, V. Linhard, D. Ludig, A. Schug, Dr. K. Saxena, Prof. Dr. H. Schwalbe
Center for Biomolecular Magnetic Resonance
Institute for Organic Chemistry and Chemical Biology
Johann Wolfgang Goethe University
Max-von-Laue-Straße 7, 60438 Frankfurt am Main (Germany)
E-mail: schwalbe@nmr.uni-frankfurt.de
Homepage: <http://schwalbe.org.chemie.uni-frankfurt.de/>

[b] Dr. M. DiPrima,⁺ Dr. G. Tosato
Laboratory of Cellular Oncology
Center for Cancer Research (CCR)
National Cancer Institute (NCI)
37 Convent Drive, NIH Bethesda Campus
Building 37, Room 4124, Bethesda, MD 20892 (USA)
E-mail: tosatog@mail.nih.gov
Homepage: <https://ccr.cancer.gov/staff-directory/giovanna-tosato>

[c] Dr. D. Kudlinzki, Dr. S. L. Gande, Prof. Dr. H. Schwalbe
German Cancer Consortium (DKTK)
German Cancer Research Center (DKFZ)
Im Neuenheimer Feld 280, 69120 Heidelberg (Germany)

[d] Dr. M. Reinecke, Dr. S. Heinzlmeir, Prof. Dr. B. Kuster
Chair of Proteomics and Bioanalytics
Technical University of Munich
Emil-Erlenmeyer-Forum 5, 85354 Freising (Germany)


[e] Dr. M. Reinecke, Prof. Dr. B. Kuster
German Cancer Consortium (DKTK)
Partner-Site Munich and German Cancer Research Center (DKFZ)
Im Neuenheimer Feld 280, 69120 Heidelberg (Germany)


[f] Dr. M. S. Leisegang
Institute for Cardiovascular Physiology
Johann Wolfgang Goethe-University
Theodor-Stern-Kai 7, 60590 Frankfurt am Main (Germany)

[g] Dr. J. Wollenhaupt, Dr. F. Lennartz, Dr. M. S. Weiss
Macromolecular Crystallography, Helmholtz-Zentrum Berlin
Albert-Einstein-Str. 15, 12489 Berlin (Germany)

[h] Prof. Dr. B. Kuster
Bavarian Center for Biomolecular Mass Spectrometry (BayBioMS)
Technical University of Munich
Emil-Erlenmeyer-Forum 5, 85354 Freising (Germany)

[*] These authors contributed equally to this work.

 Supporting information for this article is available on the WWW under <https://doi.org/10.1002/chem.202203967>

 © 2023 The Authors. Chemistry - A European Journal published by Wiley-VCH GmbH. This is an open access article under the terms of the Creative Commons Attribution License, which permits use, distribution and reproduction in any medium, provided the original work is properly cited.

the extracellular ephrin binding domain,^[8–11] 2) binding to the intracellular kinase domain.^[12–17]

In recent years, the role of EPHA2 in the development of CRC, one of the most frequently occurring cancer types,^[18] has been investigated intensively. In stage II/III CRC, EPHA2 mRNA and protein levels are abnormally elevated compared to the normal colorectal tissue and are associated with poor patient survival, raising the possibility that targeting EPHA2 might be a strategy for treatment.^[6,19] Furthermore, a significant correlation between high level expression of EPHA2 in advanced CRC and resistance to anti-epithelial growth factor receptor (EGFR) targeting with the monoclonal antibody Cetuximab has been observed.^[20,21]

Up to now, only two kinase inhibitors are FDA-approved for the treatment of metastatic CRC: 1) The multi-kinase inhibitor Regorafenib;^[22] 2) A combination of the BRAF-targeting inhibitor Encorafenib and Cetuximab for treating metastatic CRC showing a BRAF(V600E) mutation.^[23] Initial studies in CRC models showed promising effects of EPHA2 inhibition by small molecules. Specifically, the potent pan-EPH inhibitor GLPG1790 was shown to selectively target EPHA2 by reducing its phosphorylation/activation in human CRC cells and inducing cell-cycle arrest.^[24] Furthermore, ALW-II-41-27, a specific EPHA2 inhibitor, was shown to revert acquired resistance to the anti-EGFR antibody Cetuximab in human CRC models.^[25]

Previously, we performed a broad off-target analysis of pre-clinically and clinically investigated kinase inhibitors using chemical proteomics (Kinobeads technology), NMR-based conformational dynamics and crystal structures of the EPHA2-inhibitor complexes. We could identify potential scaffolds binding to EPHA2.^[26] NVP-BHG712 (NVP), a nanomolar binder of EPHB4 developed by Novartis^[27] also inhibited EPHA2 in the similar affinity regime. A detailed follow-up structural investigation revealed that all tested commercially available NVP samples were a regioisomer (NVPiso) of the originally described inhibitor by Novartis and differed in the localization of a single methyl group on the two adjacent nitrogen atoms on the pyrazole ring (Figure 1, below). This small change observed in the substitution pattern of NVP induces substantial differences not only in the binding affinities but also in the modes of binding to EPHA2 (Figure S1 in the Supporting Information).^[17] It also has varied effects on VEGF-A (vascular endothelial growth factor A)-mediated angiogenesis. Application of NVP led to a decrease of VEGF-A-mediated sprouting of human umbilical vein endothelial cells (HUVEC) as shown by a reduced number of sprouts and cumulative sprout lengths. In contrast, NVPiso did not affect VEGF-A-mediated sprouting, even at high concentrations, and Dasatinib revealed a reduction of spheroid outgrowth with increasing concentrations (Figure S2). These findings suggest that NVP and Dasatinib, but not NVPiso, exerts anti-angiogenic effects. Both isomers showed promising anti-tumor activity in human CRC, as they reduced endogenous EPH tyrosine phosphorylation, suppressed cell proliferation and increased cell death in a panel of human CRC cell lines. NVPiso additionally inhibited the growth of human CRC in mice, showing the potential of EPH inhibitors as novel therapeutics.^[28]

These findings underline that EPHA2 is a promising target for treating CRC. However, the number of studies that have focused on the development of new inhibitors for the kinase domain of EPHA2 is limited. Such inhibitors would be instrumental to gain a better understanding of the role of this specific kinase as a therapeutic target.

Results and Discussion

Based on our previous results with NVP and NVPiso, we chose to investigate this compound class from a structural, biochemical, and cellular perspective. Appreciating that even a small structural difference between NVP and NVPiso translated into substantial structural and biochemical changes, we synthesized a series of compounds featuring small modifications around the NVP and NVPiso prototypes. We introduced chemical modifications at several positions (substitution of pyridine with other azines (Figure 1; compounds 1–3), modification of the pyrazolopyrimidine moiety (compounds 4 and 5) or modifications of the phenylbenzamide motif (compounds 6–24), resulting in a series of NVP-like compounds. Furthermore, we enlarged the scope by preparing derivatives containing substructures of the kinase inhibitors Nilotinib and Ponatinib. These inhibitors are known from earlier experiments to exhibit high affinity towards EPHA2 (Kinobeads Assay: Nilotinib $K_D^{app} = 415$ nM; Ponatinib $K_D^{app} = 6.9$ nM).^[26]

For the synthesis of the NVP-like derivatives, we relied on the following synthesis sequence:^[17] 1) Preparation of the precursors (phenylbenzamides and amino modified heterocycle substructures, for detailed information see Schemes S1 and S2), and 2) Amination under Buchwald-Hartwig conditions (Scheme S3). Using this synthesis route, we could successfully prepare 24 NVP-like derivatives.

The binding affinities of these derivatives to EPHA2 were investigated by microscale thermophoresis (MST).^[29] The modification of the parent molecule NVP ($K_D = 13$ nM)^[17] causes various effects on the affinity. The introduction of different azine substituents (compounds 1 and 3) results in binding constants in the low-nanomolar range ($K_D = 3–4$ nM). In contrast, a change of the central heterocycle to a quinazoline or pyrido[2,3-*d*]pyrimidine motif leads to less potently binding inhibitors, showing an increased K_D of 86 (4) and 225 nM (5), respectively (Table 1). Modification of the phenylbenzamide moiety leads also to diverse effects on the affinities towards EPHA2. Substitutions of the CF₃-residue in the 3-position to the amide linker does not negatively influence the binding properties.

The introduction of Cl- (10), CN- (11), CH₃- (12) or OCH₃- groups (14) leads to binding constants of 2–4 nM. Only the fluorine-modified derivative 13 exhibited a slightly reduced affinity ($K_D = 32$ nM).

However, shifting the residues to the 4-position resulted in significantly less EPHA2 affine derivatives (15–18), and by introduction of larger residues like morpholine (23) and COOEt (24) the affinities were even further reduced. In contrast to this finding, derivatives featuring the optimized disubstituted

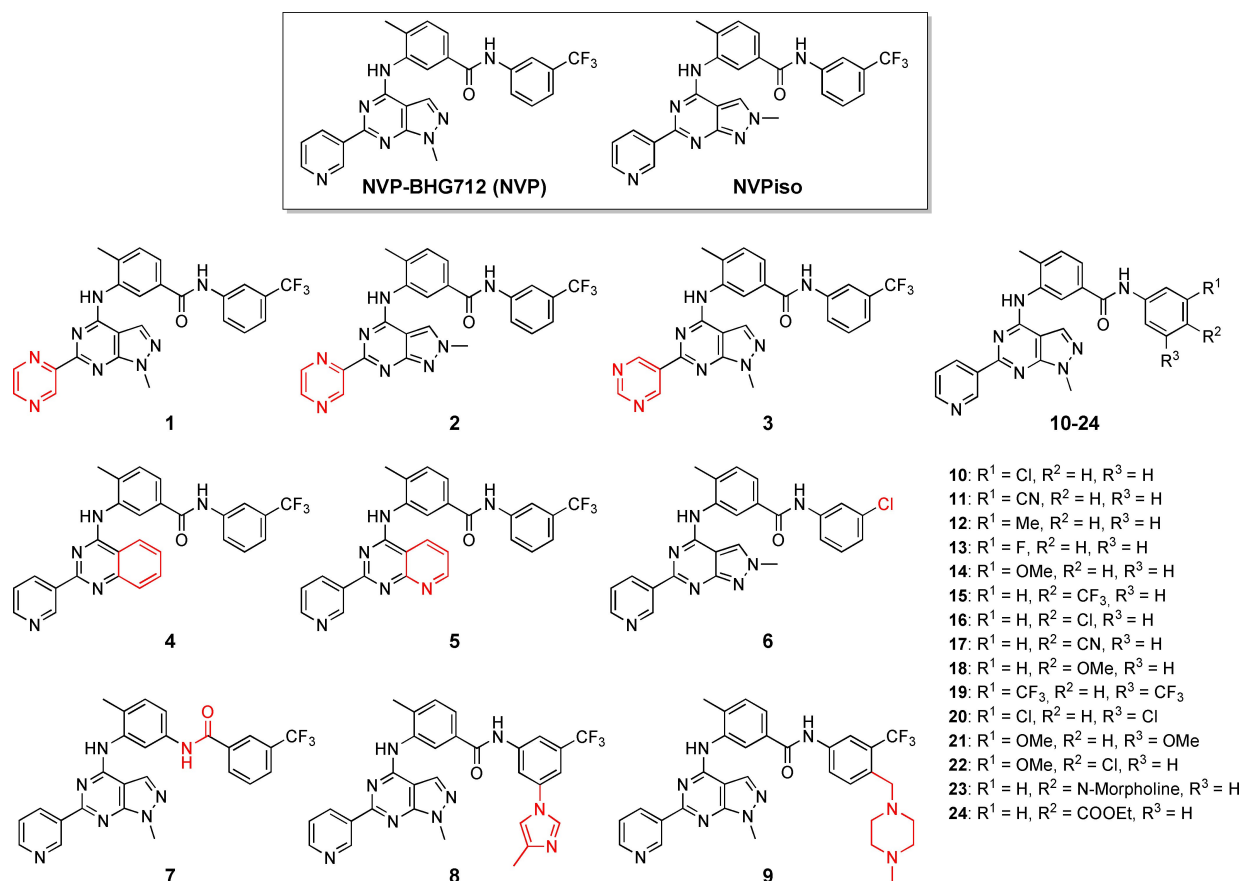


Figure 1. Chemical structures of the parent compounds NVP-BHG712 (NVP) and NVPiso as well as the synthesized NVP-like derivatives. The moieties modified in comparison to the parent compounds are marked in red.

Table 1. Affinities of the NVP-like derivatives determined by microscale thermophoresis (MST). The affinities of NVP and NVPiso were reported previously.^[17] n.i.: not inhibited.

Compound	K _D MST [nM]	Compound	K _D MST [nM]
NVP	13	12	3
NVPiso	73	13	32
1	3	14	2
2	132	15	167
3	4	16	231
4	86	17	n.i.
5	225	18	130
6	295	19	284
7	10	20	22
8	33	21	3
9	5	22	113
10	3	23	~800
11	4	24	~1000

phenylbenzamide substructures from Nilotinib and Ponatinib were well tolerated, showing high binding affinities towards EPHA2 (**8**, K_D = 33 nM and **9**, K_D = 5 nM). However, disubstituted phenylbenzamide derivatives (position 3 and 4 (**22**) or position 3 and 5 (**19–21**)) exhibited binding constants between 3 and 284 nM. The corresponding NVPiso derivatives of compound **1** and **10** showed 44- (**2**, K_D = 132 nM) and 98-fold (**6**, K_D = 295 nM), respectively, lower binding affinity towards EPHA2.

This discrepancy is in line with our previous observations for NVP and NVPiso.^[17] In summary, these results indicate that functionalization in 3-position to the phenylbenzamide bridge is more favorable than in the 4-position. Furthermore, the NVPiso-pyrazolopyrimidine motif reproducibly results in less affine derivatives in comparison to the NVP-substitution pattern.

As a next step, we co-crystallized 14 members of this series with EPHA2 to gain structural insights on how NVP substitutions affect binding modes to EPHA2. From our previous investigations, we knew that small chemical modifications of NVP can lead to different binding modes.^[17] All co-crystallized inhibitors shift the conformational equilibrium present in the apo kinase to the DFG-out conformation that is linked to an inactive state of the EPHA2 kinase. These inhibitors feature a conserved hydrogen bond interacting with the same four amino acid residues: T692 (gatekeeper), D757 (activation loop), E663 (αC helix) and M695 (hinge). Furthermore, six out of the compounds possess a dual binding mode to EPHA2. Interestingly, the heterocyclic substructure of the six NVP derivatives (**1**, **3**, **4**, **10**, **11** and **14**) adopts not only the anticipated, but also the close-to-180° rotated orientation we had previously observed in the complex of NVPiso with EPHA2 (Figure 2). This rotation around the amine axis of these compounds leads to an interaction

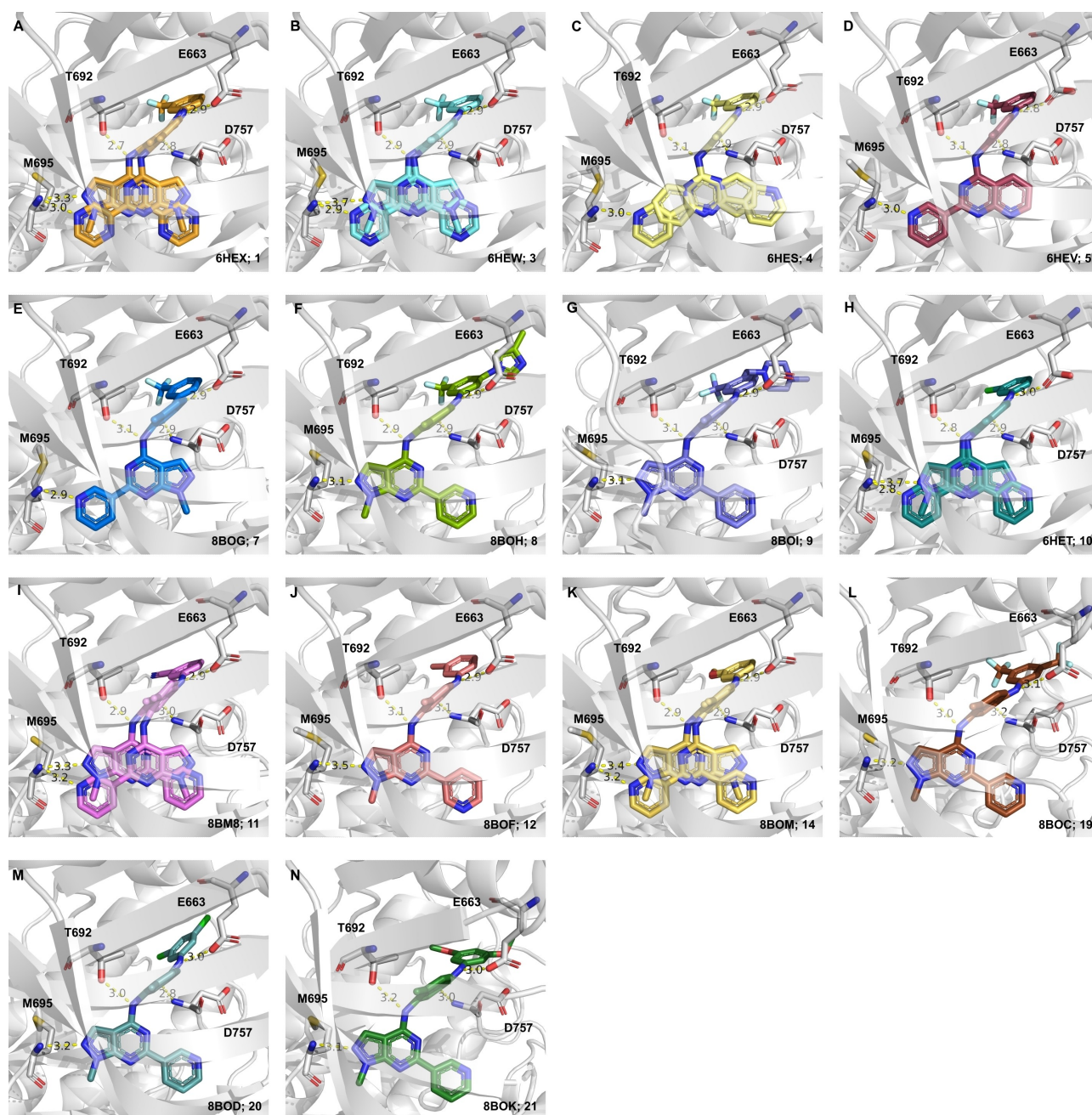


Figure 2. Crystal structures of the newly synthesized compounds in complex with EPHA2. A) 1 (PDB ID: 6HEX), B) 3 (PDB ID: 6HEW), C) 4 (PDB ID: 6HES), D) 5 (PDB ID: 6HEV), E) 7 (PDB ID: 8BOG), F) 8 (PDB ID: 8BOH), G) 9 (PDB ID: 8BOI), H) 10 (PDB ID: 6HET), I) 11 (PDB ID: 8BM8), J) 12 (PDB ID: 8BOF), K) 14 (PDB ID: 8BOM), L) 19 (PDB ID: 8BOC), M) 20 (PDB ID: 8BOD), N) 21 (PDB ID: 8BOK).

between M695 and the nitrogen of the azine substituent (NVPiso-like orientation) as well as with the pyrazole nitrogen of the pyrazolopyrimidine moiety (NVP-like orientation). A significant trend is observed by comparing inhibitor orientations in complex with EPHA2. In the case of the NVP-like orientation a short hydrogen bond towards the gatekeeper T692 (average: 2.95 Å) goes along with an elongated interaction with M695 (average: 3.22 Å) in the hinge region. In some of these structures featuring an NVP-like inhibitor orientation, the distance to M695 is too long to form a hydrogen bond.

However, the NVPiso-like orientation results in a reverse effect, that is, the hydrogen bond to M695 is shortened (average: 2.98 Å) while the interaction to the gatekeeper is elongated (average: 3.18 Å).

Surprisingly, both defined (NVP- or NVPiso-like) as well as dual binding modes could be observed for structurally similar molecules, for example compound 7, which differs from NVP only by a retro-inversed amide. Compound 7 exclusively binds to EPHA2 in an NVPiso-like orientation. Particularly unexpected, is the observation of a dual binding mode in the case of

inhibitor **4** (Figure 2C, PDB ID: 6HES), despite possessing only a single nitrogen as hydrogen bond acceptor to interact with M695. This shows that the number of formed hydrogen bonds does not seem to be decisive for the occurrence of the different binding modes. As there is no simple explanation for the observed orientations, predicting the effects of small chemical modifications on the binding mode of EPH kinase inhibitors is not straightforward, justifying a need for detailed structural analysis of similarly modified kinase inhibitors to direct the synthesis of novel inhibitors.

The dual binding mode of the NVP-derivatives in complex with EPHA2 inspired the design of symmetrically substituted triazines (**25–27**, Figure 3). The triazine core motif results from merging of the two orientations of the pyrazolopyrimidine scaffold (showing a 180° rotation, for example, present in Figure 2A and B). The aromatic substituted triazine precursors were synthesized using a one-pot ring forming reaction starting with guanidinium carbonate and aromatic nitriles (Scheme S4).^[30] We enlarged the scope of triazine derivatives also to asymmetric molecules (**28–34**) using the well-established synthesis strategy of temperature controlled nucleophilic substitutions on cyanuric chloride (Scheme S4)^[31] followed by a Buchwald-Hartwig coupling with the phenylbenzamide **S20** (Scheme S5). Using these strategies, we could prepare a series of ten triazine derivatives, which we analyzed in a next step for their affinity towards EPHA2 using MST (Table 2).

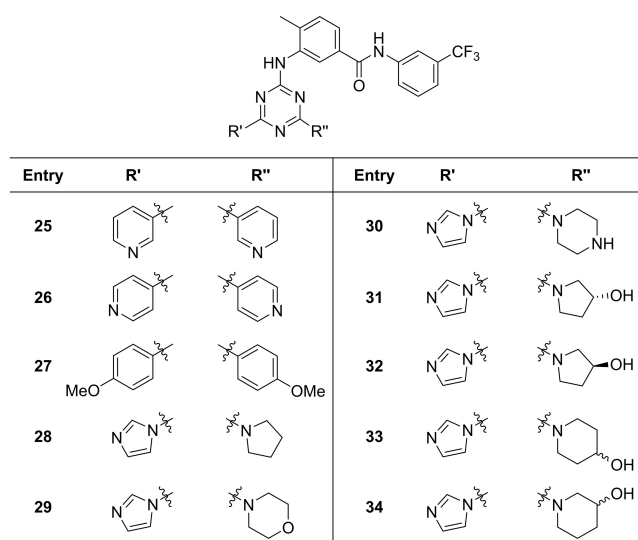


Figure 3. Chemical structures of the synthesized triazine derivatives.

Compound	K_D MST [nM]	Compound	K_D MST [nM]
25	24	30	443
26	n.i.	31	132
27	~6000	32	141
28	231	33	664
29	191	34	783

The affinities of the triazine derivatives towards EPHA2 cover a broad range from low-nanomolar to micromolar. The symmetric triazine **25**, which displays a substitution pattern (3-pyridyl) similar to the parent compound NVP, exhibit a high affinity ($K_D=24$ nM). Shifting of the pyridine substitution pattern or introduction of an anisole residue significantly reduces the affinity (**26**: not inhibited and **27**: $K_D\sim 6000$ nM). Correlation with the substitution patterns indicates that a nitrogen at position 3 of the triazine substituent is essential for generating affinity. Therefore, the asymmetric triazine derivatives are functionalized with an imidazole motif in addition to various cyclic amines. This results in affinities in the middle to high nanomolar range, whereas the hydroxypyrrolidine derivatives **31** and **32** show lowest binding constants (**31**: $K_D=132$ nM and **32**: $K_D=141$ nM). However, with the exception of the derivative **25**, the triazines appear to be less potent than the NVP-like derivatives.

We also co-crystallized the triazine series in complex with EPHA2 to obtain more structural information about the molecular interaction (Figure 4). The triazines were expected to occupy both areas in the active pocket, due to their 4,6-substitution pattern. Like the NVP-like derivatives, the co-crystallized triazines also bind to the inactive DFG-out conformation of EPHA2, stabilized by the conserved hydrogen bond pattern. An important hydrogen bond, present in all but one of the crystal structures, is formed between the amide backbone of M695 and a nitrogen atom of the pyridine or imidazole substituent, respectively. The only exception, compound **26** (Figure 4B, PDB ID: 6HEU), where this interaction cannot be detected in the crystal structure, is explained by steric hindrance from the substitution pattern preventing this interaction. These results emphasize the critical importance of a nitrogen atom as hydrogen bond acceptor in the 3-position of the substituent on the triazine core for imparting high affinity binding for the EPHA2 receptor. Two triazine derivatives also feature dual binding modes. The piperazine substituted triazine **30** (Figure S3A, PDB ID: 6Q7F) shows a second conformation resulting from a rotation of about 40° around the amine bond enabling a hydrogen bond with N744. The triazine **31** (Figure S3B, PDB ID: 6Q7E) shows that the hydroxypyrrolidine substituent adopts two orientations forming a hydrogen bond network with the amino acid residues I619, A621 and F758.

In addition to EPHA2, several other kinases play a significant role in the development and progression of CRC.^[22] To elucidate the selectivity profiles of selected compounds, including exemplary derivatives, and to identify potential off-targets of these inhibitors, we used the Kinobeads technology.^[32–35] Besides providing the isolated K_D^{app} value towards EPHA2, the Kinobeads assay gives information on the selectivity profile against broad areas of the kinome (more than 300 kinases present in different cancer cell lines), including PIKKs and PI3Ks.^[35] We could verify the general trend in affinity differences determined with MST (Figure 5 and Table S1). However, as previously observed, the measured affinity is lower in the Kinobeads assay, arising from different experimental systems, including different kinase constructs and phosphorylation states.^[17]

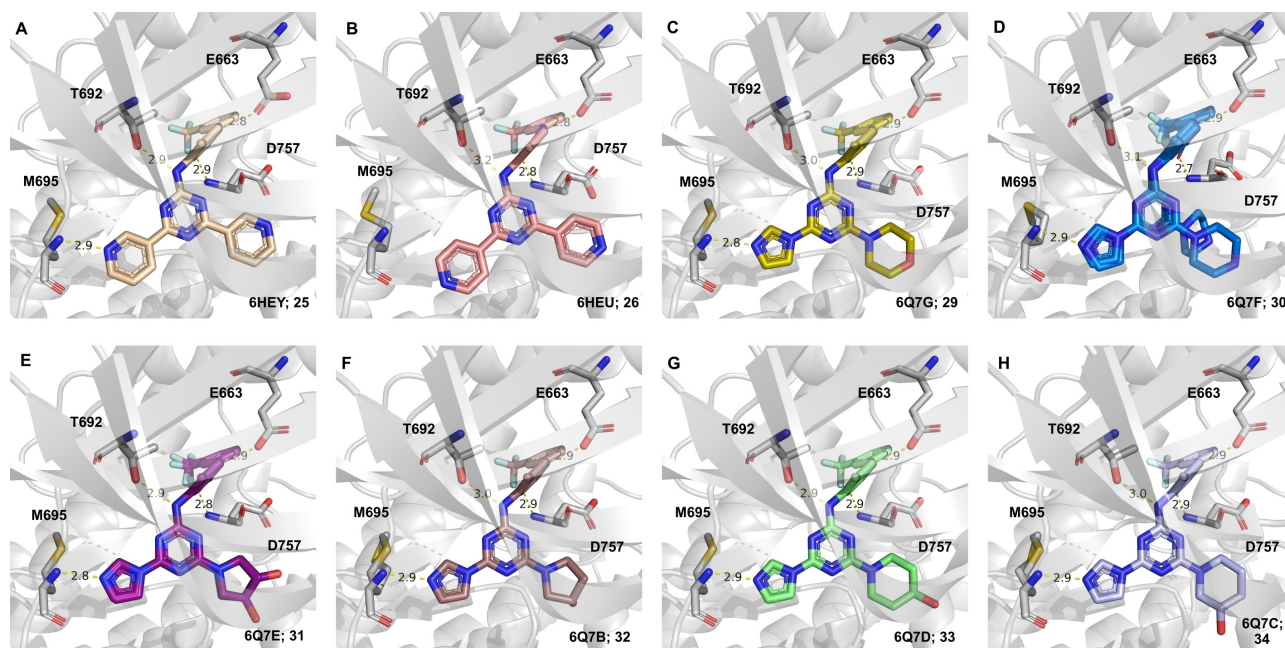


Figure 4. Crystal structures of the triazine derivatives in complex with EPHA2, the inhibitors in structures D and E adopt a dual binding mode. Crystal structures of: A) 25 (PDB ID: 6HEY), B) 26 (PDB ID: 6HEU), C) 29 (PDB ID: 6Q7G), D) 30 (PDB ID: 6Q7F), E) 31 (PDB ID: 6Q7E), F) 32 (PDB ID: 6Q7B), G) 33 (PDB ID: 6Q7D), and H) 34 (PDB ID: 6Q7C).

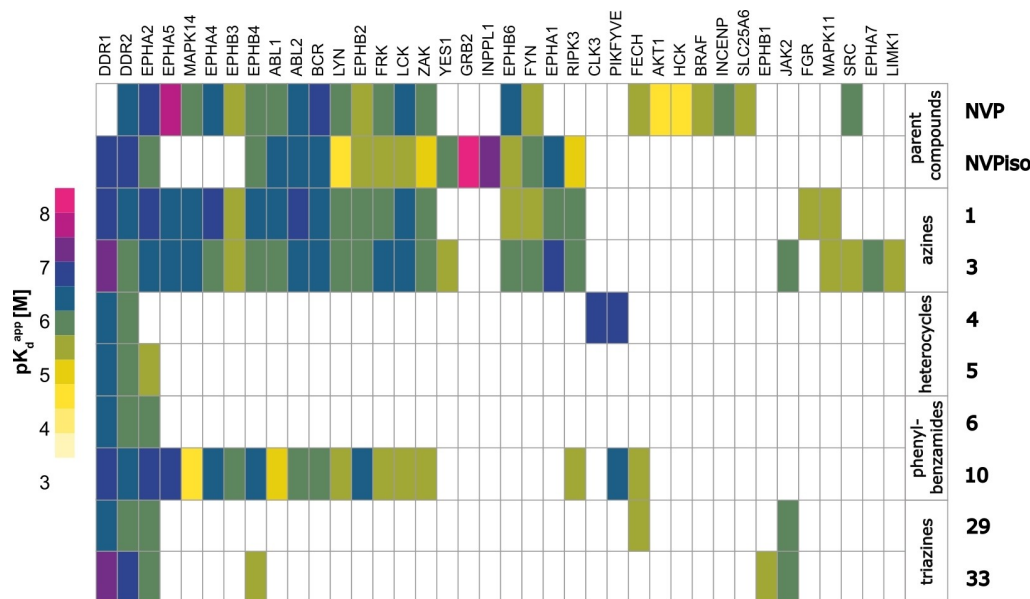


Figure 5. Selectivity profile of example derivatives (compounds 1, 3–6, 10, 29 and 33) and the parent compounds NVP and NVPiso for binding to the indicated kinases as measured by the Kinobeads assay. The color code indicates the pK_D^{app} value of the compound-target interaction. pK_D^{app} = negative logarithm of apparent dissociation constants K_D^{app} in molar. The values of NVP and NVPiso are from an earlier Kinobeads assay.^[17]

The azine substituted pyrazolopyrimidine derivatives 1 (EPHA2: $K_D^{\text{app}} = 135$ nM) and 3 (EPHA2: $K_D^{\text{app}} = 253$ nM) exhibited high-affinity binding towards several A- and B-type EPH receptors. Compared to NVP, compounds 1 and 3 displayed a somewhat different off-target profile: reduced affinity for the kinases FECH, AKT1, HCK, BRAF, INCENP and SLC25A6, and increased affinity for the kinases DDR1, EPHA1, RIPK3, and

MAPK11. Compound 1 also displayed a somewhat different off-target profile from compound 3. Modifications of the central heterocyclic motif, present in compounds 4 and 5, results in a reduction of targeted kinases, indicating more specific inhibition profiles. However, for the quinazoline 4 no binding to the EPHrin family was detected at all.

By analyzing the inhibitors **6** and **10**, we also included derivatives with modifications on the phenylbenzamide scaffold. Like the pyrazolopyrimidine derivatives **1** and **3**, compound **10** covers a broad range of the EPHrin family and further kinases (**10** (EPHA2): $K_D^{app} = 129$ nM). In comparison, the corresponding NVPiso-like derivative **6** targets EPHA2 with high selectivity, but reduced affinity ($K_D^{app} = 1477$ nM).

The triazine derivatives **29** and **33** also feature narrow selectivity profiles, showing high affinities towards the discoidin domain receptor tyrosine kinase 1 and 2 (DDR1 and DDR2). However, targeting the DDR family is a common feature of all tested inhibitors. Among the investigated NVP-like compounds, **3** revealed the highest affinity for DDR1 ($K_D^{app} = 77$ nM), while the triazine derivative **33** features a comparable affinity of $K_D^{app} = 72$ nM. This finding is in-line with our previously made observation for NVP and NVPiso^[17] and with reports noting that derivatives that bind to DDR1/2 exhibit off-target effects for the EPHrin family.^[36–39] In recent years, DDR1 and DDR2 were identified to play a role in the metastatic development in CRC and therefore, their inhibition is an attractive therapeutic strategy.^[40,41] For example, the kinase inhibitor Nilotinib, which inhibits the kinase activity of DDR1, showed a promising anti-metastatic activity in patient derived CRC cells.^[42] The observed off-target effect of the NVP derivatives, therefore, might open the opportunity to target CRC using dual inhibitors for the EPHrin and the DDR families.

We have previously demonstrated that the prototype compounds NVP and NVPiso inhibit significantly the endogenous phosphorylation of EPHB tyrosine kinase receptors expressed by human colorectal cancer cells and reduce the proliferation of human colon carcinoma cells from a panel of cell lines.^[28] Now, we initially screened the newly synthesized compounds for their ability to inhibit the spontaneous proliferation of two human colon cancer cell lines (HT-29 and SK-CO-1, Figure 6A, B) at compound concentrations ranging between 250 and 3000 nM. The HT-29 and SK-CO-1 cell lines were selected because of their high degree of sensitivity to growth inhibition by NVP and NVPiso, which were tested in parallel. Cell proliferation was measured after 72-hour exposure to the compounds or incubation in culture medium alone (control). The results of this initial screen, expressed as normalized cell proliferation, identified compounds with comparable or better inhibitory activity than NVP or NVPiso against the HT-29 and SK-CO-1 cell lines, and others with a worse inhibitory activity compared to the prototypes. In general, non-triazine derivatives performed better than triazine derivatives in this cell proliferation screen consistent with their better binding affinities to EPHA2 by MST.

Based on these initial proliferation results and consideration of EPH receptors affinity measurements (Tables 1 and 2), we selected 13 compounds (**1**, **3**, **5**, **7–15**, **29**) for further functional analyses. To this end, we selected seven human colon carcinoma cell lines that reflect the genetic, proteomic, and EPH receptors complexities of human colon carcinoma (Tables S2 and S3). All 13 compounds along with NVP and NVPiso were tested at the concentration of 1 μ M for their ability to reduce the proliferation of each of the seven cell lines. The results,

expressed as average % reduction of cell proliferation after 72-hour culture (Figure 6C), confirmed that some of the new compounds are overall comparable or better than the prototypes at inhibiting the proliferation of human colon carcinoma cells. Among the cell lines, there was variability in susceptibility to inhibition by all compounds, with some of the cell lines showing greater resistance to the inhibitors. Such resistance did not correlate with gene mutational profile (Table S2) or EPH receptors expression (Table S3) in the cell lines. In addition, some of the compounds showed increased growth inhibition for selected colon carcinoma cell lines compared to the prototypes.

Conclusion

In this study, a series of prototypically modified derivatives of the known inhibitor NVP-BHG712 as well as triazine-based molecules were synthesized and reviewed for their suitability as inhibitors of the kinase EPHA2. This included structural analysis by X-ray crystallography, biophysical determination of the affinity and selectivity for the EPH family, as well as investigation of their effect on the proliferation of different colorectal cancer cell lines. Marginal modifications of the prototypes NVP and NVPiso result in significantly different effects on the binding mode, affinity, and selectivity for EPHA2. Derivatives with a NVP-like structure prove to be particularly potent. Hereby, modifications of the azine substituent as well as substituents in position 3 to the phenylbenzamide bridge are especially suitable. In summary, these results provide evidence supporting the therapeutic potential of some of the new compounds for controlling human colon carcinoma. In addition, use of these compounds will allow fundamental research on the relationship between EPH TK inhibition, EPH receptor expression and activity, analysis of signaling pathways sustained by active TK receptors, and dissection of mechanisms underlying cell growth inhibition.

Experimental Section

Recombinant expression and purification of EPHA2 kinase domains: The gene encoding the catalytic kinase domain of human EPHA2 (D596-G900) was synthesized at GenScript USA Inc., USA, and its sequence was optimized for expression in insect cells. Synthesized EPHA2 kinase domain (EPHA2 KD) gene was subcloned in modified pTriEx 1.1-transfer vector with N-terminal Flag-His Tev protease cleavage site. Recombinant baculovirus with human EPHA2 KD was generated using BacMagicTM-3 DNA (Novagen) and pTriEx 1.1-EPHA2 KD transfer vector in insect cells by homologous recombination, according to the instructions of the BacMagic system user protocol TB459 with minor changes, as mentioned. Additional details on the recombinant EPHA2 virus generation and expression of EPHA2 KD in insect cells and purification of EPHA2 can be found in the published paper.^[43]

Protein crystallization and structure determination: EPHA2 was crystallized as previously reported.^[26,43] Diffraction data at resolutions between 0.98–1.72 Å had been collected at beamline P13^[44] (MX1) operated by the EMBL Hamburg at the PETRA III synchrotron

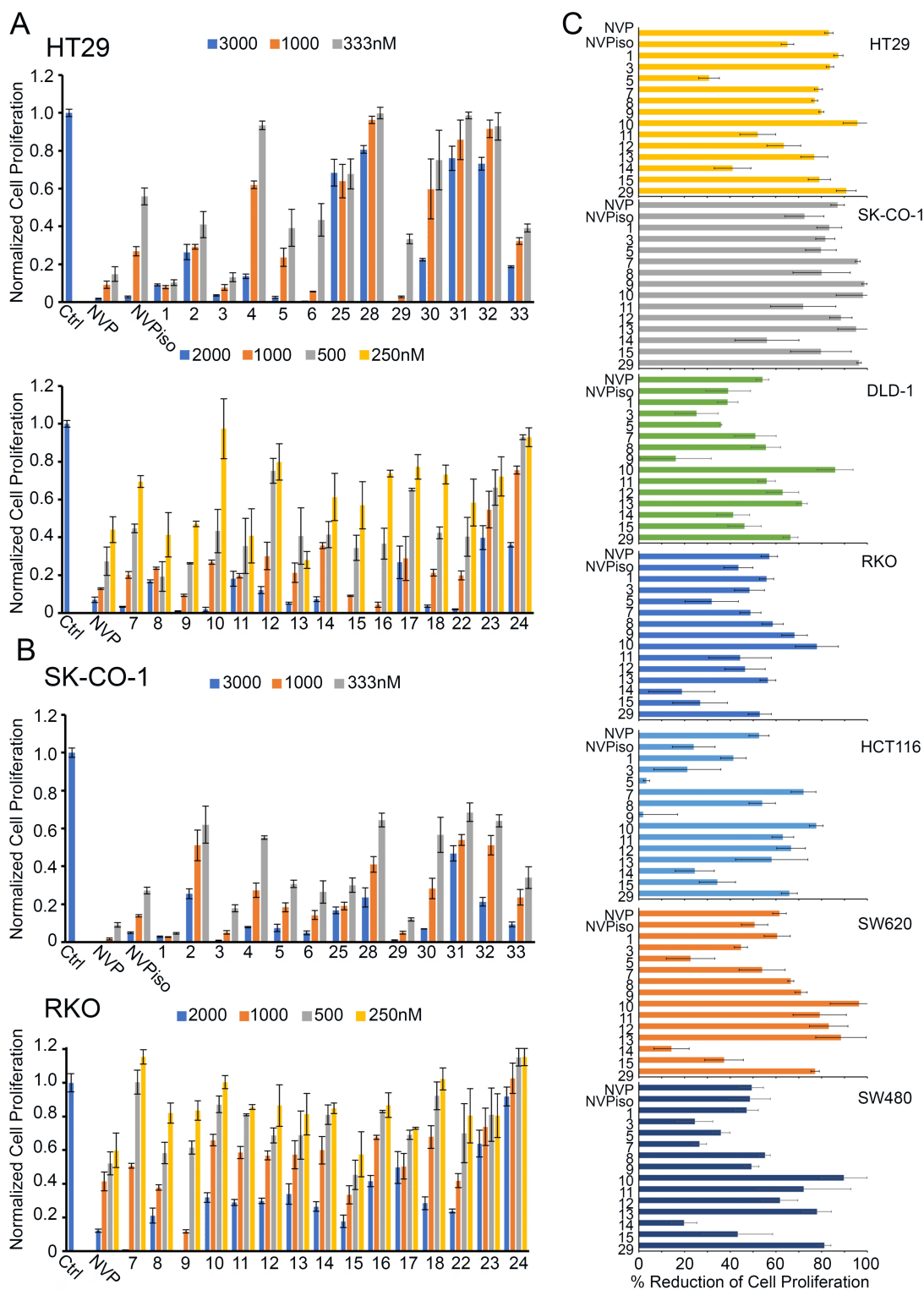


Figure 6. New compounds inhibit human colon carcinoma cell proliferation. Normalized proliferation of human colon cancer cell lines A) HT-29, B) SK-CO-1 and RKO cultured with compound or medium only for 72 h. Results from triplicate cultures (cpm \pm SEM); cpm values are normalized to the medium-only control (Ctrl). C) Normalized percentage reduction of proliferation in seven human colon cancer cell lines treated with 1 μ M compound for 72 h. cpm normalized to medium-only control. Results from $n = 2$ –6 biologic replicates \pm SEM.

source (DESY, Hamburg Germany), beamlines X06DA (PXIII) and X06SA (PXI) operated by the Swiss Light Source (PSI, Villigen,

Switzerland) and beamlines BL14.1 and BL14.2 at BESSY II operated by Helmholtz-Zentrum Berlin.^[45,46]

The data were processed by using XDSAPP.^[47] The structure was determined by molecular replacement with Phaser^[48] using the crystal structure of the human EPHA2 kinase domain bound with the ligand NVP-BHG712 (PDB ID: 6FNF)^[17] or Golvatinib (PDB ID: 5IA5)^[26] as a search model. Model building was performed using Coot^[49] and the structures were refined and validated using PHENIX.^[50] Figures containing molecular graphics were prepared by using PyMOL molecular graphics system, version 2.3.4 (Schrodinger). An overview of the structure-solution and refinement statistics can be found in the Supporting Information.

Microscale thermophoresis: The EPHA2 kinase domain (D596-G900) was fluorescently labeled using the Monolith™ Protein Labeling Kit RED-NHS (Cat# MO-L001-amine reactive) by Nanotemper according to the standard protocol. The elution of the protein was performed using the MST assay buffer (50 mM Tris pH 7.6, 150 mM NaCl, 10 mM MgCl₂, 0.05% Tween20). The MST measurement was carried out using 5% (v/v) DMSO. A 1:1 dilution series of the investigated compound was prepared (1–16, 18–25, 28–32 $c = 5 \mu\text{M}$ –0.153 nM; 27, 33, 34 $c = 50 \mu\text{M}$ –1.53 nM). After the addition of the labeled protein (final concentration 25 nM), the samples were incubated for 30 min under light exclusion at room temperature. The samples were transferred in Monolith NT.115 standard treated capillaries. The measurements were conducted using the Monolith NT.115 from Nanotemper with the following parameters: temperature: 25 °C, excitation power: 40% and MST power: 60%. The results were analyzed using MO.Affinity Analysis (version 2.1.2). All measurements were performed as duplicates. The corresponding data sets were merged, yielding an averaged curve with error bars. The used evaluation strategy was Thermophoresis with T-Jump. The measurements of the individual inhibitors are described in more detail in the Supporting Information.

Kinobeads assay

Kinase affinity pulldowns: Kinobeads pulldown experiments were performed as previously described.^[33,35] Briefly, K-562, COLO-205 and MV-4-11 cells were cultured in RPMI 1640 medium (Biochrom GmbH) supplemented with 10% (v/v) FBS (Biochrom GmbH). SK-N-BE(2) cells were grown in DMEM/Ham's F-12 (1:1) supplemented with 10% (v/v) FBS and OVCAR-8 cells were cultured in IMDM medium (Biochrom GmbH) supplemented with 10% (v/v) FBS. The cells were lysed in 0.8% NP40, 50 mM Tris-HCl pH 7.5, 5% glycerol, 1.5 mM MgCl₂, 150 mM NaCl, 1 mM Na₃VO₄, 25 mM NaF, 1 mM DTT, protease inhibitors (SigmaFast, Sigma) and phosphatase inhibitors (prepared in-house according to Phosphatase inhibitor cocktail 1, 2 and 3 from Sigma-Aldrich). The cell lysate mix used for inhibitor profiling was generated from COLO-205, K-562, SK-N-BE(2), MV-4-11 and OVCAR-8 lysates by mixing them in a 1:1:1:1:1 ratio regarding the total amount of protein as determined by Bradford. 2.5 mg of the cell lysate mixture was pre-incubated with increasing compound concentrations (DMSO vehicle, 1 nM, 3 nM, 10 nM, 30 nM, 100 nM, 300 nM, 1 μM , 3 μM , 30 μM) for 45 min at 4 °C in an end-over-end shaker. Subsequently lysates were incubated with Kinobeads (17 μL settled beads) for 30 min at 4 °C. The beads were washed and bound proteins were reduced with 50 mM DTT in 8 M urea, 40 mM Tris-HCl (pH 7.4) for 30 min at room temperature. After alkylation with 55 mM CAA proteins were digested with trypsin over night at 37 °C. Peptides were desalted and concentrated using SepPak tC18 $\mu\text{Elution}$ plates (Waters) and dried down in a SpeedVac.

LC-MS/MS analysis: Peptides were analyzed by LC-MS/MS on a Dionex Ultimate3000 nano HPLC coupled online to an Orbitrap Fusion Lumos (Thermo Fisher Scientific) mass spectrometer. Peptides were delivered to a trap column (100 $\mu\text{m} \times 2 \text{ cm}$, packed

in-house with Reprosil-Gold C₁₈ ODS-3.5 μm resin, Dr. Maisch, Ammerbuch) and washed at a flow rate of 5 $\mu\text{L min}^{-1}$ in solvent A0 (0.1% formic acid in water). Peptides were then separated on an analytical column (75 $\mu\text{m} \times 40 \text{ cm}$, packed in house with Rpsil-Gold C₁₈ 3 μm resin, Dr. Maisch, Ammerbuch) using a 52 min gradient ranging from 4–32% solvent B (0.1% formic acid, 5% DMSO in acetonitrile)^[51] in solvent A1 (0.1% formic acid, 5% DMSO in HPLC grade water) at a flow rate of 300 nL min^{-1} . The mass spectrometer was operated in a data dependent mode, automatically switching between MS1 and MS2 spectra. MS1 spectra were acquired over a mass-to-charge ratio (m/z) range of 360–1300 m/z at a resolution of 60,000 (at m/z 200) in the Orbitrap using a maximum injection time of 50 ms and an automatic gain control (AGC) target value of 4e5. Up to 12 peptide precursors were isolated (isolation width of 1.7 Th, maximum injection time of 75 ms, AGC value of 2e5), fragmented by HCD using 30% normalized collision energy (NCE) and analyzed in the Orbitrap at a resolution of 15,000. The dynamic exclusion duration of fragmented precursor ions was set to 30s.

Peptide and protein identification and quantification: Peptide and protein identification and quantification was performed using MaxQuant^[52] (v.1.6.3.3) by searching the tandem MS data against all canonical protein sequences as annotated in the UniProtKB reference database (downloaded 28.11.18, 20193 entities) using the embedded search engine Andromeda.^[53] Carbamidomethylated cysteine was set as fixed modification and phosphorylation of serine, threonine and tyrosine, oxidation of methionine and N-terminal protein acetylation as variable modifications. Trypsin/P was specified as the proteolytic enzyme and up to two missed cleavages were allowed. The minimum length of amino acids was set to seven and all data were adjusted to 1% PSM and 1% protein FDR. Label-free quantification and match between runs were enabled within MaxQuant.^[54]

Data analysis: For the Kinobeads competition binding assays, protein intensities were normalized to the respective DMSO control and IC₅₀ and EC₅₀ values were deduced by a four-parameter log-logistic regression using an internal pipeline that uses the 'drc' package in R.^[55] An apparent dissociation constant (K_D^{app}) was calculated by multiplying the estimated EC₅₀ with a protein-dependent correction factor. The correction factor of a protein is defined as the ratio of the amount of protein captured from two consecutive pulldowns of the same DMSO control lysate. Targets of the compounds were annotated manually. A protein was considered a target if the resulting binding curve showed a sigmoidal curve shape with a dose dependent decrease of binding to the beads. Additionally, the number of unique peptides and MSMS counts per condition as well as the protein intensity in the DMSO control were taken into account.

Data deposition: The mass spectrometry proteomics data and drug dose response curves have been deposited at the ProteomeX-change Consortium (<http://proteomecentral.proteomexchange.org>) through the PRIDE^[56] partner repository with the data set identifier PXD031880.

Proliferation experiments in human colon carcinoma cell lines

Cell lines: HT-29 (ATCC; HTB-38) and HCT-116 (ATCC, CCL-247) cell lines were grown in McCoy5A medium (Corning, Corning, NY; 10-050-CV) supplemented with 10% FBS (Sigma-Aldrich; F2442) and penicillin/streptomycin (ThermoFisher Scientific; 15140122); DLD-1 (ATCC, CCL-221) cell lines were grown in RPMI-1640 medium (Corning, 10-040-CV), supplemented with 10% FBS and penicillin/streptomycin; SW620 (ATCC, CCL-227), SW480 (ATCC, CCL-228), RKO (ATCC, CCL-2577), SK-CO-1 (ATCC, HTB-39), cell lines were grown in

DMEM medium (Corning, 10-017-CV), supplemented with 10% FBS and penicillin/streptomycin. Cells were only used until passage 25.

Measurement of cell proliferation: Cells were plated at 5000 cells per well (96-well flat-bottom plate) in triplicate cultures. Compounds were added at the time of plating at concentrations ranging from 250 to 3000 nM. Cell growth was measured after 72 h of incubation of cells in medium only or medium supplemented with the compounds. ³H-Tyridine (0.1 μ Ci) was added to each well and incubation continued for 8 to 10 h. Plates were frozen to stop cell growth. Plates were thawed, harvested onto glass fiber filtermats. Scintillation fluid (FiltronX National Diagnostics, Atlanta, GA, LS-201) was added to each of the filtermats and counts were measured by MicroBeta (PerkinElmer). Cell counts normalized to controls (cell counts from cells cultured in culture medium only).^[28]

All synthetic procedures and characterization data are described in the Supporting Information.

Acknowledgements

We are grateful to Drs. D. Lowy, R. Yarchoan and all members of the Laboratory of Cellular Oncology; the animal facility personnel for helping with different aspects of this project. We thank Kerstin Witt for her technical assistance and Jennifer Adam for her support in synthesis. Diffraction data were collected on beamline P13 operated by EMBL Hamburg at the PETRA III storage ring (DESY, Hamburg, Germany), beamlines X06DA (PXIII) and X06SA (PXI) operated by the Swiss Light Source (PSI, Villigen, Switzerland) and on BL14.1 and BL14.2 at the BESSY II electron storage ring operated by the Helmholtz-Zentrum Berlin and we thank the beamline staff for their support. This work was supported by the intramural program of NCI/CCR and used the computational resources of the NIH High-Performance Computing Biowulf Cluster, and by the German Consortium for Translational Cancer Research (DKTK), DFG (SFB807), and by iNEXT-Discovery, project number 871037, funded by the Horizon 2020 program of the European Commission. N.J. is supported by the DFG graduate college: CLiC. Open Access funding enabled and organized by Projekt DEAL.

Conflict of Interest

G.T., M.D., H.S., A.T., N.J. and D.K. are co-inventors on a patent application entitled "Receptor Tyrosine Kinase Inhibitors for the Treatment of Protein Kinase Modulation-responsive Disease or Disorder" (PCT/US2020/050439). The patent application was filed in part based on preliminary results related to the compounds described in the current manuscript. The invention or inventions described and claimed in this patent application were made while two of the inventors (M.D. and G.T.) were full-time employees of the U.S. Government. Under 45 Code of Federal Regulations Part 7, all rights, title, and interest to this patent application have been or should by law be assigned to the U.S. Government. The U.S. Government conveys a portion of the royalties it receives to its employee inventors under 15 U.S. Code § 3710c. B.K. is founder and shareholder of OmicScouts

GmbH and MSAID GmbH. He has no operational role in either company.

Data Availability Statement

The data that support the findings of this study are available in the supplementary material of this article.

Keywords: colorectal cancer · drug discovery · EPH receptors · medicinal chemistry · structural biology

- [1] A. Barquilla, E. B. Pasquale, *Annu. Rev. Pharmacol. Toxicol.* **2015**, *55*, 465–487.
- [2] B. C. Lechtenberg, M. P. Gehring, T. P. Light, C. R. Horne, M. W. Matsumoto, K. Hristova, E. B. Pasquale, *Nat. Commun.* **2021**, *12*, 7047.
- [3] D. P. Zelinski, N. D. Zantek, J. C. Stewart, A. R. Irizarry, M. S. Kinch, *Cancer Res.* **2001**, *61*, 2301–6.
- [4] Z. Wu, J. B. Doondeea, A. M. Gholami, M. C. Janning, S. Lemeer, K. Kramer, S. A. Eccles, S. M. Gollin, R. Grenman, A. Walch, S. M. Feller, B. Kuster, *Mol. Cell. Proteomics* **2011**, *10*, M111.011635.
- [5] J. M. Brannan, B. Sen, B. Saigal, L. Prudkin, C. Behrens, L. Solis, W. Dong, B. N. Bekele, I. Wistuba, F. M. Johnson, *Cancer Prev. Res.* **2009**, *2*, 1039–1049.
- [6] P. D. Dunne, S. Dasgupta, J. K. Blayney, D. G. McArt, K. L. Redmond, J.-A. Weir, C. A. Bradley, T. Sasazuki, S. Shirasawa, T. Wang, S. Srivastava, C. W. Ong, K. Arthur, M. Salto-Tellez, R. H. Wilson, P. G. Johnston, S. Van Schaeybroeck, *Clin. Cancer Res.* **2016**, *22*, 230–242.
- [7] W. Shen, H. Xi, K. Zhang, J. Cui, J. Li, N. Wang, B. Wei, L. Chen, *Growth Factors* **2014**, *32*, 247–253.
- [8] A. Petty, N. Idippily, V. Bobba, W. J. Geldenhuys, B. Zhong, B. Su, B. Wang, *Eur. J. Med. Chem.* **2018**, *143*, 1261–1276.
- [9] B. Wu, S. Wang, S. K. De, E. Barile, B. A. Quinn, I. Zharkikh, A. Purves, J. L. Stebbins, R. G. Oshima, P. B. Fisher, M. Pellecchia, *Chem. Biol.* **2015**, *22*, 876–887.
- [10] M. Tognolini, M. Incerti, I. Hassan-Mohamed, C. Giorgio, S. Russo, R. Bruni, B. Lelli, L. Bracci, R. Noberini, E. B. Pasquale, E. Barocelli, P. Vicini, M. Mor, A. Lodola, *ChemMedChem* **2012**, *7*, 1071–1083.
- [11] I. Hassan-Mohamed, C. Giorgio, M. Incerti, S. Russo, D. Pala, E. B. Pasquale, I. Zanotti, P. Vicini, E. Barocelli, S. Rivara, M. Mor, A. Lodola, M. Tognolini, *Br. J. Pharmacol.* **2014**, *171*, 5195–5208.
- [12] S. Heinzlmeir, J. Lohse, T. Treiber, D. Kudlinzki, V. Linhard, S. L. Gande, S. Sreeramulu, K. Saxena, X. Liu, M. Wilhelm, H. Schwalbe, B. Kuster, G. Médard, *ChemMedChem* **2017**, *12*, 999–1011.
- [13] C. J. Lim, K. Oh, J. Du Ha, J. H. Lee, H. W. Seo, C. H. Chae, D. Kim, M.-J. Lee, B. H. Lee, *Bioorg. Med. Chem. Lett.* **2014**, *24*, 4080–4083.
- [14] Y. Zhu, T. Ran, X. Chen, J. Niu, S. Zhao, T. Lu, W. Tang, *Chem. Pharm. Bull.* **2016**, *64*, 1136–1141.
- [15] V. S. Stroylov, T. V. Rikitina, F. N. Novikov, O. V. Stroganov, G. G. Chilova, A. V. Lipkin, *Mendeleev Commun.* **2010**, *20*, 263–265.
- [16] K. R. Amato, S. Wang, A. K. Hastings, V. M. Youngblood, P. R. Santapuram, H. Chen, J. M. Cates, D. C. Colvin, F. Ye, D. M. Brantley-Sieders, R. S. Cook, L. Tan, N. S. Gray, J. Chen, *J. Clin. Invest.* **2014**, *124*, 2037–2049.
- [17] A. Tröster, S. Heinzlmeir, B. Berger, S. L. Gande, K. Saxena, S. Sreeramulu, V. Linhard, A. H. Nasiri, M. Bolte, S. Müller, B. Kuster, G. Médard, D. Kudlinzki, H. Schwalbe, *ChemMedChem* **2018**, *13*, 1629–1633.
- [18] F. Bray, J. Ferlay, I. Soerjomataram, R. L. Siegel, L. A. Torre, A. Jemal, *Ca-Cancer J. Clin.* **2018**, *68*, 394–424.
- [19] H. Kataoka, H. Igarashi, M. Kanamori, M. Ihara, J.-D. Wang, Y.-J. Wang, Z.-Y. Li, T. Shimamura, T. Kobayashi, K. Maruyama, T. Nakamura, H. Arai, M. Kajimura, H. Hanai, M. Tanaka, H. Sugimura, *Cancer Sci.* **2004**, *95*, 136–141.
- [20] A. Strimpakos, G. Pentheroudakis, V. Kotoula, W. De Roock, G. Kouvatsos, P. Papakostas, T. Makatsoris, D. Papamichael, A. Andreadou, J. Sgouros, A. Zizi-Sermpetzoglou, A. Kominea, D. Televantou, E. Razis, E. Galani, D. Pectasides, S. Tejpar, K. Syrigos, G. Fountzilas, *Clin. Colorectal Cancer* **2013**, *12*, 267–274.e2.
- [21] M. Frejno, R. Zenezini Chiozzi, M. Wilhelm, H. Koch, R. Zheng, S. Klaeger, B. Ruprecht, C. Meng, K. Kramer, A. Jarzab, S. Heinzlmeir, E. Johnstone,

- E. Domingo, D. Kerr, M. Jesinghaus, J. Slotta-Huspenina, W. Weichert, S. Knapp, S. M. Feller, B. Kuster, *Mol. Syst. Biol.* **2017**, *13*, 951.
- [22] M. García-Aranda, M. Redondo, *Cancers* **2019**, *11*, 433.
- [23] S. Kopetz, A. Grothey, R. Yaeger, E. Van Cutsem, J. Desai, T. Yoshino, H. Wasan, F. Ciardiello, F. Loupakis, Y. S. Hong, N. Steeghs, T. K. Guren, H.-T. Arkenau, P. Garcia-Alfonso, P. Pfeiffer, S. Orlov, S. Lonardi, E. Elez, T.-W. Kim, J. H. M. Schellens, C. Guo, A. Krishnan, J. Dekervel, V. Morris, A. Calvo Ferrandiz, L. S. Tarpgaard, M. Braun, A. Gollerkeri, C. Keir, K. Maharry, M. Pickard, J. Christy-Bittel, L. Anderson, V. Sandor, J. Taberner, *N. Engl. J. Med.* **2019**, *381*, 1632–1643.
- [24] A. Colapietro, G. L. Gravina, F. Petragano, I. Fasciani, B. M. Scicchitano, F. Beirinckx, P. Pujuguet, L. Saniere, E. Van der Aar, D. Musio, F. De Felice, V. Mattei, S. Martellucci, R. Maggio, V. Tombolini, C. Festuccia, F. Marampon, *J. Oncol.* **2020**, *2020*, 1–16.
- [25] G. Martini, C. Cardone, P. P. Vitiello, V. Belli, S. Napolitano, T. Troiani, D. Ciardiello, C. M. Della Corte, F. Morgillo, N. Matrone, V. Sforza, G. Papaccio, V. Desiderio, M. C. Paul, V. Moreno-Viedma, N. Normanno, A. M. Rachiglio, V. Tirino, E. Maiello, T. P. Latiano, D. Rizzi, G. Signoriello, M. Sibilia, F. Ciardiello, E. Martinelli, *Mol. Cancer Ther.* **2019**, *18*, 845–855.
- [26] S. Heinzlmeir, D. Kudlinzki, S. Sreeramulu, S. Klaeger, S. L. Gande, V. Linhard, M. Wilhelm, H. Qiao, D. Helm, B. Ruprecht, K. Saxena, G. Médard, H. Schwalbe, B. Kuster, *ACS Chem. Biol.* **2016**, *11*, 3400–3411.
- [27] G. Martiny-Baron, P. Holzer, E. Billy, C. Schnell, J. Brueggen, M. Ferretti, N. Schmiedeberg, J. M. Wood, P. Furet, P. Imbach, *Angiogenesis* **2010**, *13*, 259–267.
- [28] M. DiPrima, D. Wang, A. Tröster, D. Maric, N. Terrades-Garcia, T. Ha, H. Kwak, D. Sanchez-Martin, D. Kudlinzki, H. Schwalbe, G. Tosato, *Mol. Oncol.* **2019**, *13*, 2441–2459.
- [29] M. Jerabek-Willemsen, T. André, R. Wanner, H. M. Roth, S. Dühr, P. Baaske, D. Breitsprecher, *J. Mol. Struct.* **2014**, *1077*, 101–113.
- [30] “Triazine mit Andenosin antagonistischer Wirkung”, U. Kuefner-Muehl, S. W. Scheuplein, G. Pohl, W. Gaida, E. Lehr, J. Mierau, C. J. M. Meade, DE19735800 A1, **1997**.
- [31] G. Blotny, *Tetrahedron* **2006**, *62*, 9507–9522.
- [32] G. Médard, F. Pachel, B. Ruprecht, S. Klaeger, S. Heinzlmeir, D. Helm, H. Qiao, X. Ku, M. Wilhelm, T. Kuehne, Z. Wu, A. Dittmann, C. Hopf, K. Kramer, B. Kuster, *J. Proteome Res.* **2015**, *14*, 1574–1586.
- [33] S. Klaeger, S. Heinzlmeir, M. Wilhelm, H. Polzer, B. Vick, P.-A. Koenig, M. Reinecke, B. Ruprecht, S. Petzoldt, C. Meng, J. Zecha, K. Reiter, H. Qiao, D. Helm, H. Koch, M. Schoof, G. Canevari, E. Casale, S. R. Depaolini, A. Feuchtinger, Z. Wu, T. Schmidt, L. Rueckert, W. Becker, J. Huenges, A.-K. Garz, B.-O. Gohlke, D. P. Zolg, G. Kayser, T. Voeder, R. Preissner, H. Hahne, N. Tönisson, K. Kramer, K. Götz, F. Bassermann, J. Schlegl, H.-C. Ehrlich, S. Aiche, A. Walch, P. A. Greif, S. Schneider, E. R. Felder, J. Ruland, G. Médard, I. Jeremias, K. Spiekermann, B. Kuster, *Science* **2017**, *358*, eaan4368.
- [34] M. Bantscheff, D. Eberhard, Y. Abraham, S. Bastuck, M. Boesche, S. Hobson, T. Mathieson, J. Perrin, M. Rida, C. Rau, V. Reader, G. Sweetman, A. Bauer, T. Bouwmeester, C. Hopf, U. Kruse, G. Neubauer, N. Ramsden, J. Rick, B. Kuster, G. Drewes, *Nat. Biotechnol.* **2007**, *25*, 1035–1044.
- [35] M. Reinecke, B. Ruprecht, S. Poser, S. Wiechmann, M. Wilhelm, S. Heinzlmeir, B. Kuster, G. Médard, *ACS Chem. Biol.* **2019**, *14*, 655–664.
- [36] Y. Choi, F. Syeda, J. R. Walker, P. J. Finerty, D. Cuerrier, A. Wojciechowski, Q. Liu, S. Dhe-Paganon, N. S. Gray, *Bioorg. Med. Chem. Lett.* **2009**, *19*, 4467–4470.
- [37] H. Terai, L. Tan, E. M. Beauchamp, J. M. Hatcher, Q. Liu, M. Meyerson, N. S. Gray, P. S. Hammerman, *ACS Chem. Biol.* **2015**, *10*, 2687–2696.
- [38] D. E. Jeffries, C. M. Borza, A. L. Blobaum, A. Pozzi, C. W. Lindsley, *ACS Med. Chem. Lett.* **2020**, *11*, 29–33.
- [39] Z. Wang, Y. Zhang, D. M. Pinkas, A. E. Fox, J. Luo, H. Huang, S. Cui, Q. Xiang, T. Xu, Q. Xun, D. Zhu, Z. Tu, X. Ren, R. A. Brekken, A. N. Bullock, G. Liang, K. Ding, X. Lu, *J. Med. Chem.* **2018**, *61*, 7977–7990.
- [40] A. Sirvent, M. Lafitte, S. Roche, *Mol. Cell Oncol.* **2018**, *5*, 4, DOI: 10.1080/23723556.2018.1465882.
- [41] M. Lafitte, A. Sirvent, S. Roche, *Front. Oncol.* **2020**, *10*, 25, DOI: 10.3389/fonc.2020.00125.
- [42] M. Jeitany, C. Leroy, P. Tosti, M. Lafitte, J. Le Guet, V. Simon, D. Bonenfant, B. Robert, F. Grillet, C. Mollevi, S. El Messaoudi, A. Otandault, L. Canterel-Thouennon, M. Busson, A. R. Thierry, P. Martineau, J. Pannequin, S. Roche, A. Sirvent, *EMBO Mol. Med.* **2018**, *10*, e7918.
- [43] S. L. Gande, K. Saxena, S. Sreeramulu, V. Linhard, D. Kudlinzki, S. Heinzlmeir, A. J. Reichert, A. Skerra, B. Kuster, H. Schwalbe, *ChemBioChem* **2016**, *17*, 2257–2263.
- [44] M. Cianci, G. Bourenkov, G. Pompidor, I. Karpics, J. Kallio, I. Bento, M. Roessle, F. Cipriani, S. Fiedler, T. R. Schneider, *J. Synchrotron Radiat.* **2017**, *24*, 323–332.
- [45] M. Gerlach, U. Mueller, M. S. Weiss, *J. large-scale research facilities JLSRF* **2016**, *2*, A47.
- [46] U. Mueller, R. Förster, M. Hellmig, F. U. Huschmann, A. Kastner, P. Malecki, S. Pühringer, M. Röwer, K. Sparta, M. Steffien, M. Ühlein, P. Wilk, M. S. Weiss, *Eur. Phys. J. Plus* **2015**, *130*, 141.
- [47] M. Krug, M. S. Weiss, U. Heinemann, U. Mueller, *J. Appl. Crystallogr.* **2012**, *45*, 568–572.
- [48] A. J. McCoy, R. W. Grosse-Kunstleve, P. D. Adams, M. D. Winn, L. C. Storoni, R. J. Read, *J. Appl. Crystallogr.* **2007**, *40*, 658–674.
- [49] P. Emsley, K. Cowtan, *Acta Crystallogr. Sect. D* **2004**, *60*, 2126–2132.
- [50] P. v. Afonine, R. W. Grosse-Kunstleve, N. Echols, J. J. Headd, N. W. Moriarty, M. Mustyakimov, T. C. Terwilliger, A. Urzhumtsev, P. H. Zwart, P. D. Adams, *Acta Crystallogr. Sect. D* **2012**, *68*, 352–367.
- [51] H. Hahne, F. Pachel, B. Ruprecht, S. K. Maier, S. Klaeger, D. Helm, G. Médard, M. Wilm, S. Lemeer, B. Kuster, *Nat. Methods* **2013**, *10*, 989–991.
- [52] J. Cox, M. Mann, *Nat. Biotechnol.* **2008**, *26*, 1367–1372.
- [53] J. Cox, N. Neuhauser, A. Michalski, R. A. Scheltema, J. v. Olsen, M. Mann, *J. Proteome Res.* **2011**, *10*, 1794–1805.
- [54] J. Cox, M. Y. Hein, C. A. Luber, I. Paron, N. Nagaraj, M. Mann, *Mol. Cell. Proteomics* **2014**, *13*, 2513–2526.
- [55] C. Ritz, J. C. Streibig, *J. Stat. Softw.* **2005**, *12*, 1–18.
- [56] J. A. Vizcaino, R. G. Côté, A. Csordas, J. A. Dianes, A. Fabregat, J. M. Foster, J. Griss, E. Alpi, M. Birim, J. Contell, G. O’Kelly, A. Schoenegger, D. Ovelleiro, Y. Pérez-Riverol, F. Reisinger, D. Ríos, R. Wang, H. Hermjakob, *Nucleic Acids Res.* **2013**, *41*, 1063–1069.

Manuscript received: December 19, 2022

Accepted manuscript online: February 17, 2023

Version of record online: March 22, 2023